Membrane protein recycling from the vacuole/lysosome membrane

Sho W. Suzuki and Scott D. Emr

The lysosome (or vacuole in yeast) is the central organelle responsible for cellular degradation and nutrient storage. Lysosomes receive cargo from the secretory, endocytic, and autophagy pathways. Many of these proteins and lipids are delivered to the lysosome membrane, and some are degraded in the lysosome lumen, whereas others appear to be recycled through unknown pathways. In this study, we identify the transmembrane autophagy protein Atg27 as a physiological cargo recycled from the vacuole. We reveal that Atg27 is delivered to the vacuole membrane and then recycled using a two-step recycling process. First, Atg27 is recycled from the vacuole to the endosome via the Snx4 complex and then from the endosome to the Golgi via the retromer complex. During the process of vacuole-to-endosome retrograde trafficking, Snx4 complexes assemble on the vacuolar surface and recognize specific residues in the cytoplasmic tail of Atg27. This novel pathway maintains the normal composition and function of the vacuole membrane.

Introduction

Most membrane proteins are initially synthesized at the ER membrane and then sorted to their proper destination (i.e., plasma membrane, Golgi, lysosome, etc.) via vesicle trafficking pathways (Schekman, 1985). In budding yeast, the transmembrane protein receptor for carboxypeptidase Y (CPY), Vps10, sorts CPY into vesicles at the Golgi (Marcusson et al., 1994). After CPY-containing vesicles are transported to the endosome, the endosome matures and fuses with the vacuole, delivering soluble CPY to the vacuole lumen. Unlike CPY, Vps10 is not delivered to the vacuole, but is recycled from the endosome back to the Golgi by the retromer complex before fusion with the vacuole. Retromer is a conserved protein complex responsible for membrane protein retrieval (Cullen, 2008) that is composed of Vps5, Vps17, Vps26, Vps29, and Vps35 in yeast (Horazdovsky et al., 1997; Seaman et al., 1997, 1998). It deforms the endosomal membrane to form cargo-containing recycling tubules/vesicles, which give rise to recycling vesicles that fuse with the Golgi, where Vps10 can be reused for another round of CPY sorting. In mammalian cells, Snx1/2 (Vps5 homologue) and Snx5/6 (Vps17 homologue) form a complex, which mediates retrograde traffic of the mannose-6-phosphate receptor (M6PR; Kvainickas et al., 2017; Simonetti et al., 2017).

Sorting nexins (SNXs) are an evolutionarily conserved protein family comprising a Phox homology (PX) domain that binds to phosphatidylinositol 3-phosphate (PI3P), allowing its selective interaction with endosomes (Carlton et al., 2005). Most SNXs also possess a Bin-amphiphysin-Rvs167 (BAR) domain that induces/stabilizes membrane curvature. These SNXs have been classified as the SNX-BAR subfamily (Cullen, 2008). Previous studies have identified 8 yeast and 12 mammalian SNX-BAR proteins, including the retromer subunits Vps5 and Vps17 (Horazdovsky et al., 1997; Seaman et al., 1997, 1998). Snx4 forms a complex with either Snx41 or Snx42 and mediates the recycling of the v-SNARE Snc1 in yeast (Hettema et al., 2003) and the transferrin receptor in mammalian cells (Traer et al., 2007). It has been shown that SNXs are linked to disease (i.e., Alzheimer's disease) and pathogenic infection (Cullen, 2008).

Atg27 is a type I transmembrane protein, which localizes at the Golgi to function in autophagy during the biogenesis of Atg9 vesicles (Fig. 1 A; Yamamoto et al., 2012; Backues et al., 2015). Atg9 vesicles are essential for autophagosome formation (Yamamoto et al., 2012). Atg27 possesses an M6PR fold in its lumenal region (Fig. 1 A and see Discussion). In the process of Atg9 vesicle biogenesis, Atg27 binds Atg9 via this M6PR fold (Legakis et al., 2007). In atg27Δ cells, the number of Atg9 vesicles decreases, resulting in a defect in autophagy and in the cytoplasm-to-vacuole targeting (Cvt) pathway, a selective type of autophagy (Yen et al., 2007). A recent study reports that Atg27 also localizes to the vacuole membrane and is delivered via the AP-3 pathway independent of Atg9 vesicle biogenesis or autophagy (Fig. S1 A; Segarra et al., 2015). It possesses a tyrosine-based motif (268-YSAV-271), which interacts with the AP-3 coat complex (Fig. 1 A), and mutations in this motif abrogate the vacuole localization of Atg27.

Weill Institute for Cell and Molecular Biology and Department of Molecular Biology and Genetics, Cornell University, Ithaca, NY.

Correspondence to Scott D. Emr: sde26@cornell.edu.
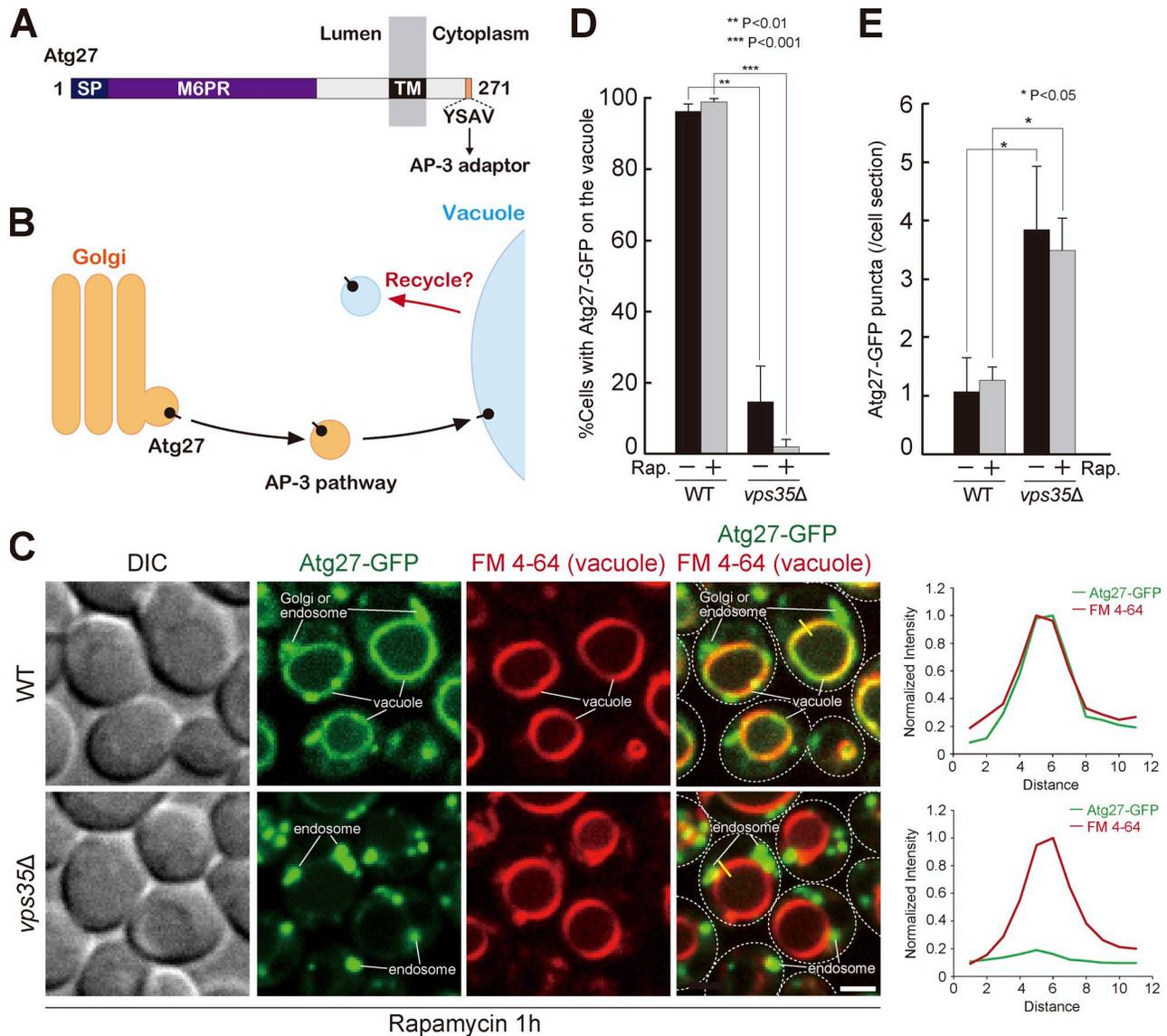
Figure 1. **Atg27 accumulates on endosomes in retromer mutants. (A)** Schematic of Atg27. **(B)** Hypothesis for Atg27 trafficking. **(C)** Atg27-GFP localization after 1 h of rapamycin treatment. Line scan analysis was performed for the region highlighted by the yellow line. DIC, differential interference contrast. **(D)** Percentage of cells with Atg27-GFP on the vacuole. **(E)** Number of Atg27-GFP puncta per cell, from C and Fig. S1 B. For all quantification shown in this figure, at least 100 cells were measured, and the data from three independent experiments were used for statistical analysis; two-tailed Student's *t* test. Error bars represent SD. Bar, 2 µm.

The lysosome (or vacuole in yeast and plants) is responsible for the degradation of cellular proteins delivered by autophagy or the multivesicular body (MVB) pathway and also serves as a reservoir for catabolic products (i.e., amino acids, ions, sugars, and fatty acids; Mizushima et al., 2011; Perera and Zoncu, 2016). Lysosomes constantly receive new membrane and membrane proteins through fusion with AP-3 vesicles, autophagosomes, and endosomes, which must be degraded or recycled to maintain lysosome homeostasis. To investigate lysosomal membrane protein recycling, we used *Saccharomyces cerevisiae* as a model. We found that the transmembrane protein Atg27 is recycled from the vacuole to the endosome via the Snx4 complex and then from the endosome to the Golgi by the retromer complex. We propose that the Snx4 complex plays a critical role in membrane protein retrieval from the vacuole membrane.

Results and discussion

Atg27 accumulates on the endosome in retromer mutants

To characterize how membrane proteins are recycled off the vacuole, we examined the transmembrane protein Atg27, which is delivered to the vacuole membrane via the AP-3 pathway (Fig. 1, A and B; and Fig. S1 A). When we expressed Atg27-GFP from its native promoter in WT cells, it mainly localized on the vacuole membrane (Fig. S1 B). It also localized on several punctate structures, which were previously reported to be the Golgi or endosomes (Segarra et al., 2015).

Genome-wide analysis suggests that several retromer complex subunits physically interact with Atg27 (Tarassov et al., 2008). Hence, we examined Atg27 localization in a retromer mutant. In the retromer-defective *vps35Δ* strain, Atg27-GFP localized on the vacuole membrane (Fig. 1 D and Fig. S1 B), and the number
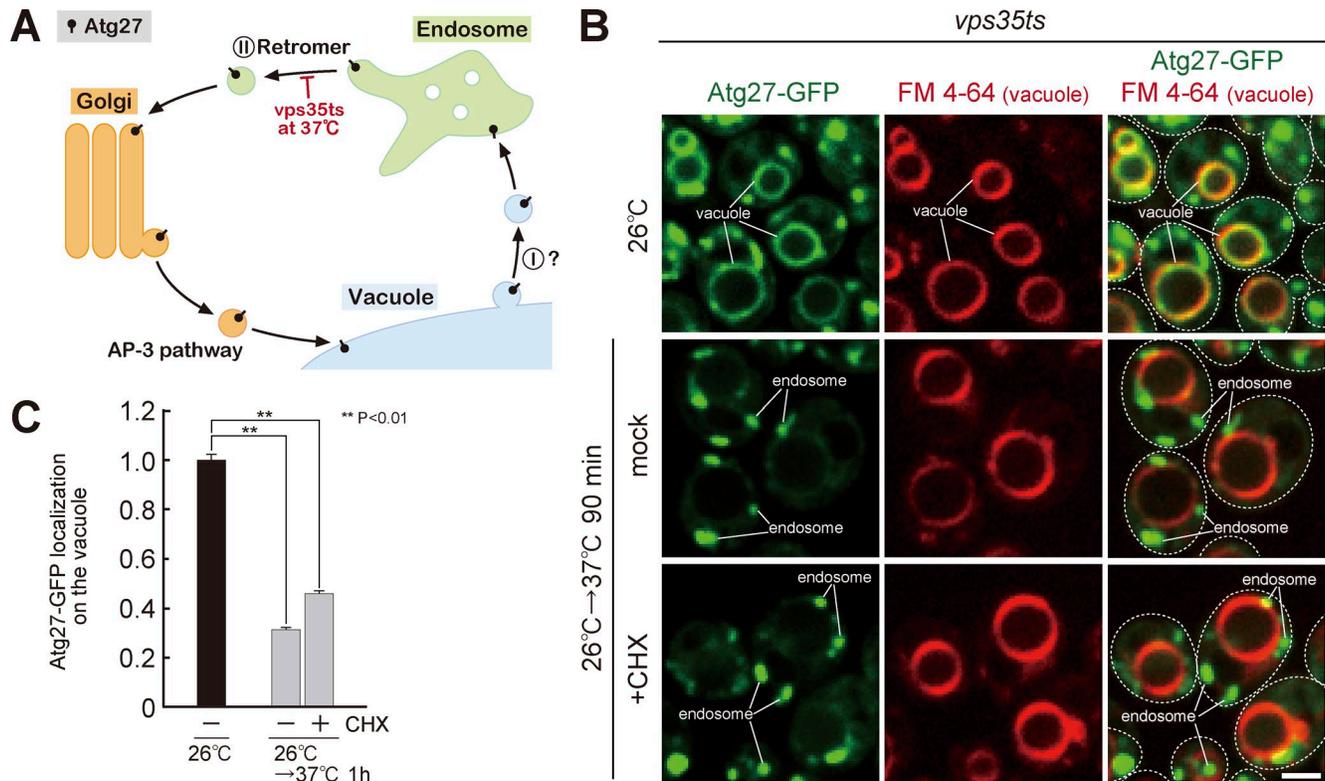
Figure 2. **Atg27 is recycled from the vacuole membrane to the endosome. (A)** Hypothesis for Atg27 trafficking. **(B)** Atg27-GFP localization in *vps35ts* after shift to 37°C with rapamycin and CHX treatment. **(C)** Quantification of Atg27-GFP fluorescence intensity on the vacuole. For all quantification shown in this figure, at least 100 cells were measured, and the data from three independent experiments were used for statistical analysis; two-tailed Student's *t* test. Error bars represent SD. Bar, 2 μm.

of cellular punctate structures increased (Fig. 1 E and Fig. S1 B). Because Atg27-mediated Atg9 vesicle biogenesis is stimulated during autophagy (Yamamoto et al., 2012), we treated yeast cells with the TORC1 inhibitor rapamycin and found a stronger *vps35Δ*-dependent defect in Atg27-GFP localization (Fig. 1, C–E). Thus, we hereafter decided to observe Atg27-GFP localization in rapamycin-treated cells. Atg27-GFP localization was similarly affected in *vps29Δ* cells (Fig. S1 C). The V-ATPase subunit Vph1 remained stably localized on the vacuole membrane in rapamycin-treated *vps35Δ* cells (Fig. S1 D), suggesting that the Atg27-GFP localization defect is specific. We found that Atg27-GFP puncta frequently colocalized with Nhx1-2XmCherry rather than Sec7-mCherry (Fig. S1, E–G), demonstrating that Atg27 accumulates on the endosome in retromer mutants.

Atg27 is recycled from the vacuole membrane using a two-step recycling process

Atg27 is directly delivered from the Golgi to the vacuole membrane via the AP-3 pathway, not through the endosome (Fig. S1 A). However, in retromer mutants, Atg27 accumulated on the endosome (Fig. 1 C and Fig. S1 E). Based on these observations, we hypothesized that after the delivery to the vacuole membrane, Atg27 is recycled to the endosome by an unknown pathway and then retrieved from the endosome to the Golgi by the retromer complex (Fig. 2 A). To test this, we analyzed Atg27-GFP localization in a *vps35ts* mutant. At 26°C, Atg27-GFP was stably localized on the vacuole membrane (Fig. 2, B and C); however, after

shifting to 37°C, Atg27-GFP accumulated on endosomes and was depleted from the vacuole membrane. In contrast, the temperature shift did not affect Atg27-GFP localization in WT cells (Fig. S1 H). We also treated *vps35ts* cells with cycloheximide (CHX) to inhibit new protein synthesis, and Atg27-GFP still shifted from vacuoles to endosomes at 37°C (Fig. 2, B and C), suggesting that the endosomal Atg27-GFP is not newly synthesized and is caused by a lack of retromer function (Fig. 2 A). Collectively, we propose the following Atg27 trafficking model: (1) Atg27 is delivered from the Golgi to the vacuole membrane via the AP-3 pathway. (2) Then, it is recycled from the vacuole membrane to the endosome by an unknown pathway. (3) Finally, Atg27 is retrieved from the endosome to the Golgi by the retromer complex.

The Snx4 complex mediates Atg27 vacuole-to-endosome retrograde transport

We sought to identify the machinery responsible for the vacuole-to-endosome transport of Atg27. Membrane protein recycling is mainly facilitated by SNXs, so we tested whether SNX proteins mediate vacuole-to-endosome retrograde trafficking of Atg27-GFP. Because Atg27-GFP accumulates on endosomes in *vps35Δ* cells (Fig. 1 C), we hypothesized that mutating the genes required for Atg27 retrieval from the vacuole in a *vps35Δ* mutant would cause Atg27-GFP to remain on the vacuole (Fig. 3 A). We analyzed Atg27-GFP localization in cells lacking *VPS35* and each of the SNXs (Fig. 3 B and Fig. S2 A) and found that Atg27-GFP localized on the vacuole membrane in *vps35Δ snx4Δ* cells (Fig. 3,

B and C). We also observed a small population of Atg27-GFP on the endosome (Fig. S2 B), suggesting that Atg27 vacuole-to-endosome transport is not completely blocked in *vps35Δ snx4Δ* cells. To directly test whether Snx4 is required for vacuole-to-endosome transport, we analyzed Atg27-GFP localization in *vps35ts snx4Δ* cells and found that it remained on the vacuole membrane after shifting to 37°C (Fig. 3, D and E), but accumulated on endosomes in *vps35ts SNX4* cells at 37°C (Fig. 3 E and Fig. S2 C). We also confirmed that Atg27-GFP localized on the vacuole membrane in *snx4Δ* cells (Fig. S2 D). Thus, Snx4 is required for the vacuole-to-endosome retrograde transport of Atg27.

Snx4 forms a complex with Snx41 or Snx42, which is required for its membrane localization (Ma et al., 2017). We tested whether Snx41 and Snx42 also affect Atg27 vacuole-to-endosome retrograde traffic. In both *vps35Δ snx41Δ* and *vps35Δ snx42Δ* cells, Atg27-GFP localized to endosomes (Fig. 3 C). However, in *vps35Δ snx41Δ/42Δ* cells, Atg27-GFP was stably localized on the vacuole membrane. In *vps35Δ snx4Δ/41Δ/42Δ* cells, Atg27-GFP also localized on the vacuole membrane, suggesting that Snx41 and Snx42 function is redundant. We conclude that Snx4 forms a complex with either Snx41 or Snx42 to recycle Atg27 from the vacuole.

To address whether the Snx4 complex recognizes Atg27, we performed a coimmunoprecipitation experiment. When we immunoprecipitated Atg27-GFP, Snx4-3XHA coprecipitated (Fig. 3 F). This Atg27–Snx4 interaction was still observed in *snx41Δ/42Δ* cells (Fig. S2 E). These data suggest that Snx4 physically interacts with Atg27.

The PI3P binding and the BAR domain of Snx4 are required for Atg27 vacuole-to-endosome retrograde transport

Snx4 comprises an N-terminal PX domain and a C-terminal BAR domain, which are required for PI3P binding and membrane deformation, respectively (Fig. 4 A). We analyzed the requirement for these domains in vacuole-to-endosome retrograde traffic of Atg27. Atg27-GFP remained on the vacuole membrane in cells expressing Snx4^{ΔPX} or Snx4^{ΔBAR} (Fig. 4, A and B; and Fig. S2 F), suggesting that both the PX and BAR domains are required for Atg27 retrieval.

The PI 3-kinase Vps34 synthesizes PI3P (Schu et al., 1993). To test the requirement of PI3P for Atg27 retrieval, we examined Atg27-GFP localization in *vps35Δ vps34ts* cells. At 37°C, Atg27-GFP remained on the vacuole membrane (Fig. 4 C), demonstrating that PI3P is required for Atg27 retrieval, but not for delivery to the vacuole membrane. Blocking Vps34 activity also prevents the synthesis of PI(3,5)P$_2$, which is synthesized from PI3P by Fab1 (Cooke et al., 1998; Gary et al., 1998). Thus, we tested Atg27-GFP localization in *vps35Δ fab1ts* cells. Atg27-GFP was still able to accumulate on endosomes at 37°C (Fig. 4 D), indicating that PI(3,5)P$_2$ is dispensable for Atg27 vacuole-to-endosome transport. Collectively, these data indicate that Atg27 vacuole-to-endosome retrograde transport requires both the PI3P binding and the membrane-deforming activity of the Snx4 complex.

Multiple Snx4 complexes assemble on the vacuole membrane in a PI3P-dependent manner

Next, we examined the localization of the Snx4 complex. Snx4-GFP formed several punctate structures proximal to the vacuole membrane (Fig. 4, E and G; and Fig. S2 G). Because the yeast vacuole membrane contains PI3P (Cheever et al., 2001; Zhu et al., 2017), we tested whether Snx4-GFP punctate localization requires PI3P. Snx4-GFP punctate localization was abolished in *vps34ts* cells after shifting to 37°C (Fig. S2 H). The Snx4 complex is known to localize on the endosomal membrane and contributes to Snc1 endosome-to-Golgi retrograde traffic (Hettema et al., 2003). Because endosomes localize close to the vacuole membrane, it is difficult to determine whether the Snx4-GFP puncta are localized on the endosome or the vacuole membrane. To distinguish this, we examined the colocalization of Snx4-GFP with Nhx1-2XmCherry, which localizes on endosomes. We found that ∼70% of Snx4-GFP punctate structures colocalize with Nhx1-2XmCherry (Fig. 4, F [open arrowheads] and H), but the remaining ∼30% of Snx4-GFP puncta did not (Fig. 4, F [closed arrowheads] and I), indicating that they may be assembling on the vacuole membrane. Snx4-GFP puncta that did not colocalize with Nhx1-2XmCherry increased upon rapamycin treatment (Fig. 4, F and I; and Fig. S2 I), consistent with the observation that rapamycin treatment induces Atg27 trafficking from the vacuole to the endosome. Endosome formation requires the t-SNARE Pep12 and the Sec1/Munc-18 family protein Vps45 (Becherer et al., 1996; Burd et al., 1997). Hence, we also examined Snx4-GFP localization in *pep12Δ* or *vps45Δ* cells and found that Snx4-GFP still formed several punctate structures in these mutants (Fig. 4 J). Snx4-3XHA also associated with purified vacuoles (Fig. S2 J). Atg27-GFP punctate structures on the vacuole membrane colocalized with Snx4-DsRed (Fig. 4 K). Based on these observations, Snx4 complexes assemble on both the vacuole and endosomal membranes in a PI3P-dependent manner.

The cytoplasmic tail of Atg27 is required for its vacuole-to-endosome retrograde transport

Finally, we analyzed which residues of Atg27 are required for vacuole-to-endosome retrograde transport, focusing on the C-terminal cytoplasmic tail. To ensure vacuole delivery of the Atg27 tail truncations, we fused a dileucine AP-3 recognition motif to Atg27, Atg27-diL-GFP (Fig. 5 A). Atg27-diL-GFP localized on the vacuole membrane similarly to Atg27-GFP and shifted to the endosome in *vps35Δ* mutants (Fig. 5, B and C). In *vps35Δ snx4Δ* cells, Atg27-diL-GFP remained on the vacuole membrane, suggesting that the retrograde trafficking of Atg27-diL-GFP is similar to WT Atg27-GFP. We then truncated the cytoplasmic tail of Atg27 (Fig. S3 A). In WT cells, Atg27^{ΔC}-diL-GFP was localized on the vacuole membrane (Fig. S3 B) and remained on the vacuole membrane in *vps35Δ* cells, suggesting that the cytoplasmic tail of Atg27 is required for its vacuole-to-endosome retrograde transport.

Next, we examined which residues are required for the vacuole-to-endosome retrograde transport of Atg27 by generating a series of mutants, each having five consecutive amino acids replaced with alanine (Fig. 5 A). Mutating a 15–amino acid sequence in the cytoplasmic tail (residues 222–237) strongly blocked vacuole-to-endosome trafficking (Fig. 5 A and Fig. S3 C). We then mutated single residues in this region to alanine. All of the mutant proteins expressed well except G226A. We found that only R224A, S227A, F231A, and I236A exhibited defects in
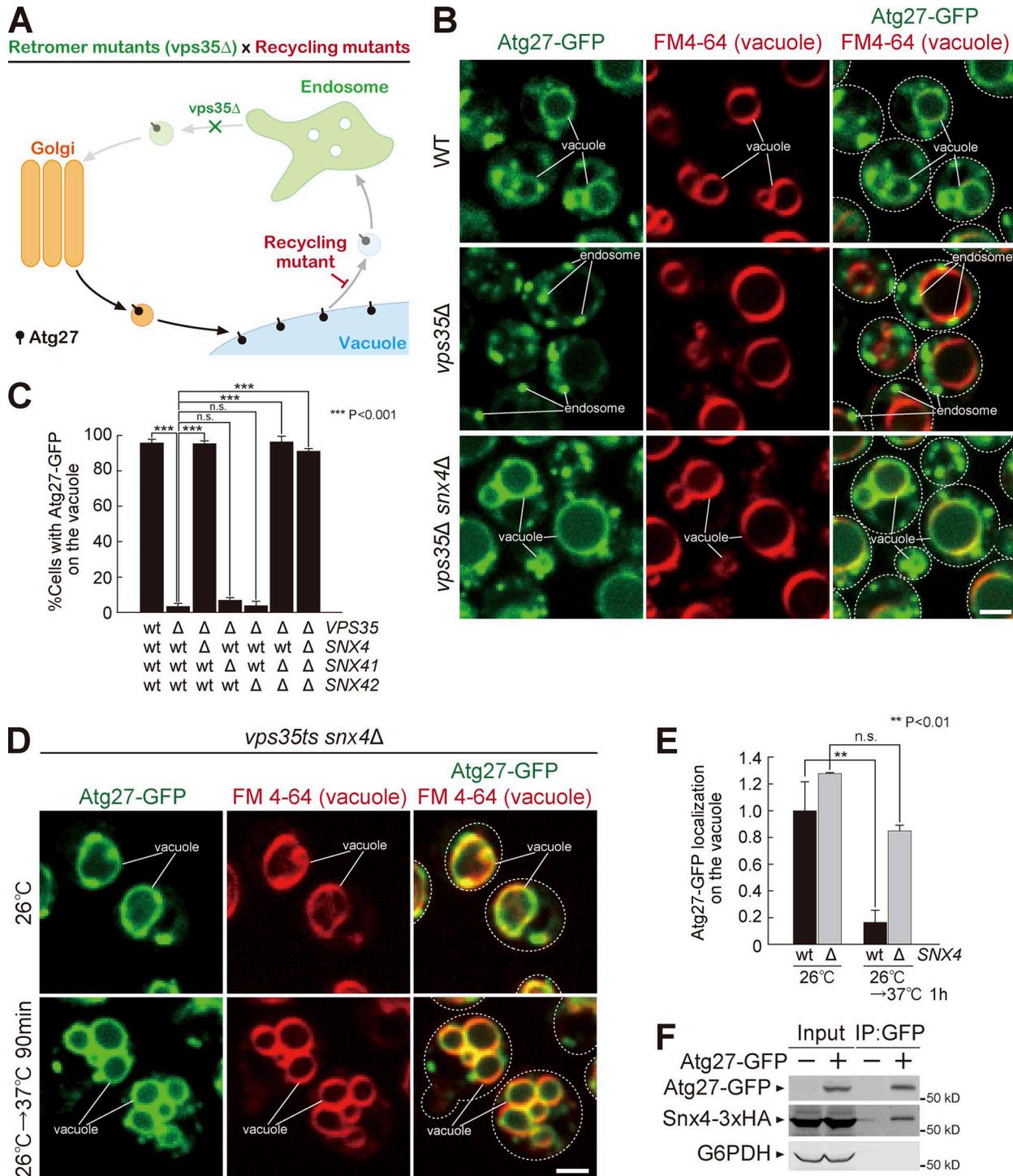
Figure 3. **The Snx4 complex mediates Atg27 vacuole-to-endosome retrograde transport. (A)** Schematic predicting Atg27 accumulation on the vacuole membrane in retromer and recycling double mutants. **(B)** Atg27-GFP localization in *vps35Δ snx4Δ* cells after 1 h of rapamycin treatment. **(C)** The percentage of cells with Atg27-GFP on the vacuole. **(D)** Atg27-GFP localization in *vps35ts snx4Δ* mutants after shift to 37°C with rapamycin treatment for 1 h. **(E)** Quantification of Atg27-GFP fluorescence intensity on the vacuole from D and Fig. S2 C. **(F)** Cells were treated with rapamycin for 1 h, Atg27-GFP was immunoprecipitated, and interacting Snx4-3XHA was detected by immunoblot. For all quantification shown in this figure, at least 100 cells were measured, and the data from three independent experiments were used for statistical analysis; two-tailed Student's *t* test. Error bars represent SD. IP, immunoprecipitation; n.s., not significant. Bar, 2 µm.

vacuole-to-endosome traffic (Fig. 5, D and E; and Fig. S3 D). To test whether these residues are required for Snx4 binding, we examined the Atg27–Snx4 interaction. We found that R224A reduced the affinity with Snx4 (Fig. 5 F). These results suggest that the cytoplasmic tail of Atg27 is required for its vacuole-to-endosome retrograde transport.
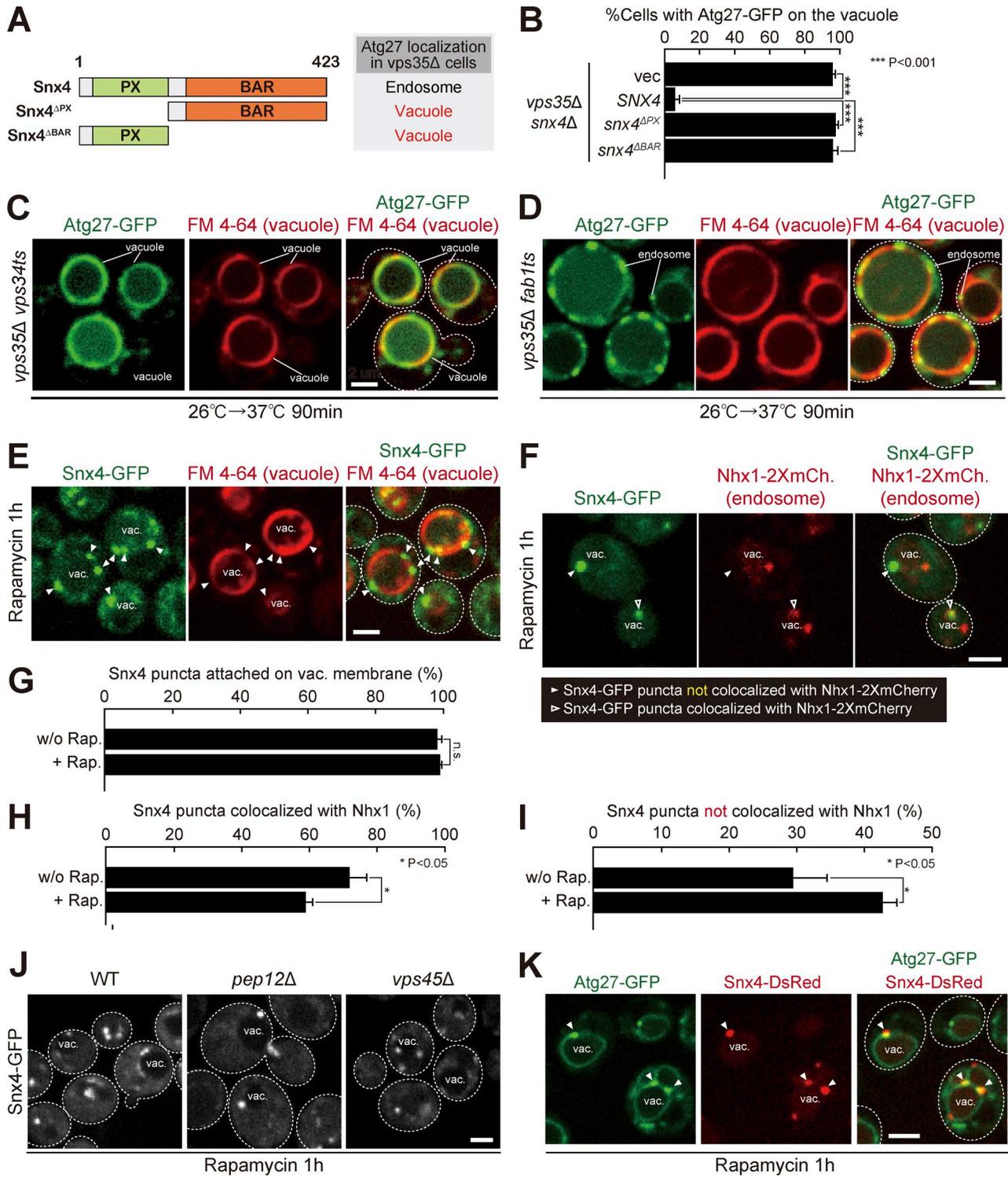
Figure 4. **Multiple Snx4 complexes assemble on the vacuole membrane in a PI3P-dependent manner. (A)** Schematic of Snx4 domains. **(B)** The percentage of *vps35Δ* cells with Atg27-GFP on the vacuole when expressing *snx4* mutants after 1 h of rapamycin treatment, from Fig. S2 F. **(C and D)** Atg27-GFP localization in *vps35Δ vps34ts* (C) and *vps35Δ fab1ts* (D) after shifting to 37°C with rapamycin for 90 min. **(E and F)** Snx4-GFP colocalization with FM 4–64 (E) and Nhx1 (F) after 1 h of rapamycin treatment. Arrowheads in E indicate Snx4-GFP punctate structures. Open arrowheads and closed arrowheads in F show Snx4-GFP puncta that are colocalized and not colocalized with the endosome (Nhx1-2XmCherry), respectively. **(G)** Quantification of Snx4-GFP punctate structures on the vacuole membrane from E and Fig. S2 G. **(H and I)** Quantification of Snx4-GFP punctate structures on (H) and off (I) the endosome from F and Fig. S2 I. **(J)** Snx4-GFP localization in *pep12Δ* and *vps45Δ* mutants after 1 h of rapamycin treatment. **(K)** Atg27-GFP colocalization with Snx4-DsRed after 1 h of rapamycin treatment. Arrowheads indicate colocalized Atg27-GFP and Snx4-DsRed. For all quantification shown in this figure, at least 100 cells were measured, and the data from three independent experiments were used for statistical analysis; two-tailed Student's *t* test. Error bars represent SD. n.s., not significant. Bars, 2 μm.
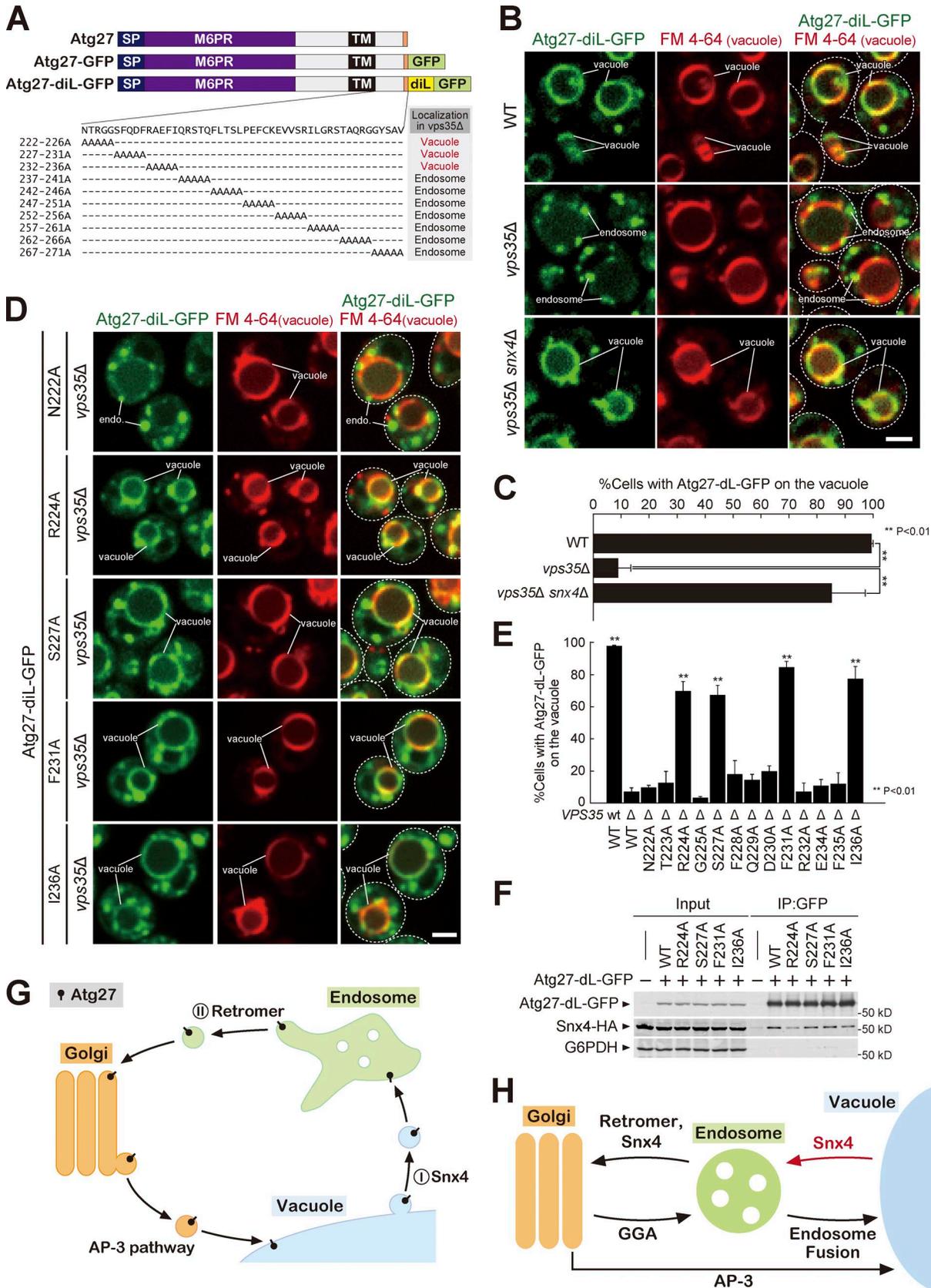
Figure 5. **Specific residues in the cytoplasmic tail of Atg27 are required for its retrograde traffic. (A)** Schematic of Atg27 mutational analysis from Fig. S3 C. **(B)** Atg27-diL-GFP localization after 1 h of rapamycin treatment. **(C)** The percentage of cells with Atg27-diL-GFP on the vacuole in B. **(D)** Atg27-diL-GFP mutant localization in *vps35Δ* cells after 1 h of rapamycin treatment. **(E)** The percentage of cells with Atg27-diL-GFP on the vacuole in D and Fig. S3 D. **(F)** Cells

In this study, we reveal that Atg27 is recycled from the vacuole membrane by a two-step recycling process (Fig. 5 G). During vacuole-to-endosome retrograde transport, Snx4 complexes assemble on the vacuole membrane in a PI3P-dependent manner. The Snx4 complex recognizes and sorts Atg27 by physically interacting with the cytoplasmic tail of Atg27. The Snx4 BAR domains deform the vacuole membrane to form recycling vesicles/tubules containing Atg27. At present, how these vesicles/tubules selectively recognize and fuse with the endosome, and the identity of additional components of the sorting machinery, remains unknown.

Previously, retention sequence–alkaline phosphatase (RS-ALP), which fused a retromer retrieval signal to ALP (Pho8 in yeast), was reported to be delivered from the vacuole membrane to the endosome (Bryant et al., 1998). However, the addition of the DPAP-A retrieval motif onto ALP removed the dileucine motif, which is essential for the vacuole localization via the AP-3 pathway (Darsow et al., 1998). Hence, it remains unclear how/whether RS-ALP is delivered to the vacuole membrane and how it is retrieved from the vacuole membrane. Our study identified Atg27 as the first physiological substrate for vacuole-to-endosome retrograde transport. Retrieval of RS-ALP from the vacuole membrane requires $PI(3,5)P_2$ (Bryant et al., 1998), but Atg27 recycling does not, suggesting that Atg27 retrograde trafficking is distinct from that of RS-ALP.

A recent study reported that Snx4 is required for endosome-to-Golgi retrograde traffic of Atg27 (Ma et al., 2017). They showed that Atg27$^{\Delta YSAV}$-GFP, lacking the tyrosine-based motif required for vacuole localization (Segarra et al., 2015), is localized on the Golgi in WT cells but on the vacuole membrane in $snx4\Delta$ cells. From these results, they concluded that the endosome-to-Golgi retrograde transport of Atg27 requires Snx4. However, WT Atg27 is directly delivered to the vacuole membrane via the AP-3 pathway without trafficking through the endosome (Fig. S1 A; Segarra et al., 2015). Hence, this study did not address the complete trafficking route for Atg27. Here, we reveal that the Snx4 complex is required for the retrograde transport of Atg27 from the vacuole membrane. Indeed, Atg27 accumulates on the endosome in retromer mutants despite functional Snx4 (Hettema et al., 2003), suggesting that Snx4 recycles Atg27 from the vacuole membrane, not from the endosome.

The vacuole-to-endosome transport of Atg27 is enhanced by rapamycin treatment (Fig. 1 D), but it is unclear why the retrieval of Atg27 is up-regulated. It is reported that Atg9 vesicle biogenesis from the Golgi is stimulated during autophagy induction, which requires the Golgi-localized Atg27 (Yamamoto et al., 2012). Activation of the vacuole-to-endosome transport might increase Atg27 population on the Golgi. Further investigation will be necessary to resolve this issue.

Our mutational analysis revealed that R224, S227, F231, and I236 on the cytoplasmic tail of Atg27 are required for its retrograde transport. Interestingly, other Snx4 cargoes (Snc1, Ste6, and Sft2; Krsmanovic et al., 2005; Bean et al., 2017) contain similar sequences in their cytoplasmic region (Fig. S3 E), providing a mechanism for Snx4 cargo recognition. Further investigation will be necessary to fully characterize the detailed sequence constraints on the Snx4 complex sorting signal.

Interestingly, Snx4, Snx41, and Snx42 are conserved in mammalian cells as HsSnx4, HsSnx7, and HsSnx30, respectively (Fig. S3 F; Cullen, 2008), raising the possibility that retrograde traffic from the lysosomal membrane to the endosome is conserved in mammalian cells. Importantly, HsSnx4 mutations are associated with certain forms of breast cancer (Shah et al., 2009).

Recycling of membrane and key proteins (SNAREs, receptors, etc.) allows cells to maintain organelle identity. In this study, we reveal that the Snx4 complex mediates membrane protein recycling from the vacuole membrane (Fig. 5 H). Several other SNXs might also function in this pathway. It will be important to address the role for each SNX and identify their specific cargoes to fully understand how cells maintain the composition and function of each organelle.

Materials and methods

Yeast strain and plasmid
S. cerevisiae strains used in this study are listed in Table S1. Plasmids used in this study are listed in Table S2. Standard protocols were used for yeast manipulation (Kaiser et al., 1994). Cells were cultured at 30°C to mid-log phase in YPD medium (1% [wt/vol] yeast extract, 2% [wt/vol] bacto peptone, and 2% [wt/vol] glucose) or YNB medium (0.17% [wt/vol] yeast nitrogen base without amino acids and ammonium sulfate, 0.5% [wt/vol] ammonium sulfate, and 2% [wt/vol] glucose) and supplemented with the appropriate nutrients. For the temperature-sensitive mutants, cells were grown to mid-log phase at 26°C and then were shifted to 37°C. To inactivate TORC1, cells were treated with 0.2 µg/ml rapamycin. To inhibit new protein synthesis, cells were treated with 50 µg/ml CHX. The functionality of Atg27-GFP was confirmed by Ape1 delivery to the vacuole (Fig. S3 G; Legakis et al., 2007).

Preparation of yeast cell lysate
Cell lysates were prepared as follows: cells were grown to mid-log phase at 30°C. Aliquots of cells were mixed with trichloroacetic acid at a final concentration of 15%, and the mixtures were incubated for 30 min at 4°C. After centrifugation at 17,400 *g* for 10 min at 4°C, the cells were washed once with 100% acetone and then were lysed in SDS-PAGE sample buffer (60 mM Tris-HCl, pH 7.5,

were treated with rapamycin for 1 h and Atg27-diL immunoprecipitated. Interacting Snx4-3XHA mutants were detected by immunoblotting. **(G)** Model for Atg27 trafficking. Atg27 is delivered to the vacuole membrane via the AP-3 pathway and then recycled from the vacuole membrane to the endosome by the Snx4 complex. Atg27 is then retrieved from the endosome by retromer. **(H)** Membrane trafficking pathways in yeast cells. For all quantification shown in this figure, at least 100 cells were measured, and the data from three independent experiments were used for statistical analysis; two-tailed Student's *t* test. Error bars represent SD. IP, immunoprecipitation. Bars, 2 µm.

2% [wt/vol] SDS, 10% glycerol, 100 mM DTT, and bromophenol blue) by beading with 0.5 mm YZB zirconia beads (Yasui Kikai) for 2 min. The lysates were then heated at 98°C for 5 min. After centrifugation at 10,000 g for 1 min at RT, supernatants were analyzed by SDS-PAGE and immunoblotting using anti-GFP and anti-Pgk1.

Antibodies

For immunoblotting, mouse anti-GFP (clone 7.1/13.1; Roche), mouse anti-Pgk1 antibody (no. 459250; Invitrogen), mouse anti-HA (12CA5; Roche), rabbit anti-G6PDH (Sigma-Aldrich), and mouse anti-ALP (459260; NOVEX) were purchased and used at dilution factors of 1:1,000, 1:5,000, 1:1,000, 1:20,000, and 1:500, respectively.

Immunoprecipitation

To examine the Snx4–Atg27 interaction, cells expressing Atg27-GFP and Snx4-3XHA were grown to mid-log phase at 30°C and were treated with rapamycin for 1 h before harvest. Cells were washed twice with wash buffer (50 mM Tris-HCl, pH 8.0, 150 mM NaCl, and 10% glycerol). The cells were lysed in immunoprecipitation buffer (50 mM Tris-HCl, pH 8.0, 150 mM NaCl, 10% glycerol, 1 mM PMSF, and 1× protease inhibitor cocktail [Roche]) and lysed by beating with 0.5 mm YZB zirconia beads for 60 min. Immunoprecipitation buffer containing 0.2% Triton X-100 was added to the lysate (final concentration of 0.1%), and the samples were rotated at 4°C for 10 min. The solubilized lysates were cleared at 500 g for 5 min at 4°C, and the resultant supernatants were subjected to a high-speed centrifugation at 17,400 g for 10 min. The cleared supernatants were incubated with preequilibrated GFP-TRAP_A beads (Chromo Tek) and rotated at 4°C for 4 h. After the beads were washed with wash buffer containing 0.1% Triton X-100, the bound proteins were eluted by incubating the beads in SDS-PAGE sample buffer at 98°C for 5 min.

Fluorescence microscopy

Fluorescence microscopy was performed using a CSU-X spinning-disk confocal microscopy system (Intelligent Imaging Innovations) with a DMI 6000B microscope (Leica), 100×/1.45 numerical aperture objective, and a QuantEM electron-multiplying charge-coupled device camera (Photometrics). Imaging was done at RT in YNB medium using GFP and mCherry channels with different exposure times according to the fluorescence intensity of each protein. Images were analyzed and processed with SlideBook 6.0 software (Intelligent Imaging Innovations).

Quantitative analysis of Atg27-GFP on the vacuole membrane

The ImageJ program (National Institutes of Health) was used to process images. To quantify the degree of colocalization between Atg27-GFP and the vacuole membrane marker FM 4–64, the JACoP plugin was used to generate Manders' coefficients (Bolte and Cordelières, 2006). For each experiment, at least 100 cells were measured, and the data from three independent experiments were used for statistical analysis. Error bars were obtained from three individual experiments. *, P < 0.05; **, P < 0.01; and ***, P < 0.001 by two-tailed Student's t test. In Fig. 2 C, the mean intensity of Atg27-GFP in *vps35ts* cells at 26°C is set to 1.0. In Fig. 3 E, the mean intensity of Atg27-GFP in *vps35ts snx4Δ* cells at 26°C is set to 1.0.

Purification of vacuoles

Vacuoles were purified as described previously with some modifications (Ohsumi and Anraku, 1981). In short, cells expressing Snx4-3XHA were grown to log phase (OD$_{600}$ = 0.8) at 30°C and were harvested by centrifugation at 4,500 g for 3 min. Cells were washed with washing buffer (0.1 M Tris-HCl, pH 8.0, and 10 mM DTT) and resuspended in spheroplasting buffer (0.5× YPD, 0.8 M sorbitol, and 1.0 mg/ml zymolyase). Cells were incubated at 30°C for 60 min to be converted to spheroplasts. The spheroplasts were washed with ice-cold buffer A (20 mM Hepes-KOH, pH 7.2, and 1.2 M sorbitol) and then resuspended in ice-cold buffer B (10 mM Pipes-KOH, pH 6.8, 0.2 M sorbitol, and 15% Ficoll). Cells were homogenized by the Dounce homogenizer and centrifuged twice at 500 g for 5 min. The supernatants were transferred to SW40 tubes. Then, ice-cold buffer C (10 mM Pipes-KOH, pH 6.8, 0.2 M sorbitol, and 8% Ficoll] was layered. We centrifuged at 110,000 g for 90 min at 4°C and collected vacuoles from the top layer. Vacuoles were mixed with trichloroacetic acid at a final concentration of 15%, and the mixtures were incubated for 30 min at 4°C. After centrifugation at 17,400 g for 10 min at 4°C, vacuoles were washed once with 100% acetone and then incubated with SDS-PAGE sample buffer at 98°C for 5 min. Prepared samples were analyzed by SDS-PAGE and immunoblotting using anti-ALP, anti-HA, and anti-G6PDH.

Online supplemental material

Fig. S1 shows that Atg27 accumulates on the endosome in retromer mutants. Fig. S2 shows that the Snx4 complex mediates Atg27 vacuole-to-endosome retrograde transport. Fig. S3 shows that the cytoplasmic tail of Atg27 is required for its vacuole-to-endosome retrograde transport. Table S1 shows yeast strains used in this study. Table S2 shows plasmids used in this study.

References

Backues, S.K., D.P. Orban, A. Bernard, K. Singh, Y. Cao, and D.J. Klionsky. 2015. Atg23 and Atg27 act at the early stages of Atg9 trafficking in S. cerevisiae. *Traffic.* 16:172–190. https://doi.org/10.1111/tra.12240

Bean, B.D., M. Davey, and E. Conibear. 2017. Cargo selectivity of yeast sorting nexins. *Traffic.* 18:110–122. https://doi.org/10.1111/tra.12459

Becherer, K.A., S.E. Rieder, S.D. Emr, and E.W. Jones. 1996. Novel syntaxin homologue, Pep12p, required for the sorting of lumenal hydrolases to the lysosome-like vacuole in yeast. *Mol. Biol. Cell.* 7:579–594. https://doi.org/10.1091/mbc.7.4.579

Bolte, S., and F.P. Cordelières. 2006. A guided tour into subcellular colocalization analysis in light microscopy. *J. Microsc.* 224:213–232. https://doi.org/10.1111/j.1365-2818.2006.01706.x

Bryant, N.J., R.C. Piper, L.S. Weisman, and T.H. Stevens. 1998. Retrograde traffic out of the yeast vacuole to the TGN occurs via the prevacuolar/endosomal compartment. *J. Cell Biol.* 142:651–663. https://doi.org/10.1083/jcb.142.3.651

Burd, C.G., M. Peterson, C.R. Cowles, and S.D. Emr. 1997. A novel Sec18p/NSF-dependent complex required for Golgi-to-endosome transport in yeast. *Mol. Biol. Cell.* 8:1089–1104. https://doi.org/10.1091/mbc.8.6.1089

Carlton, J., M. Bujny, A. Rutherford, and P. Cullen. 2005. Sorting nexins--unifying trends and new perspectives. *Traffic.* 6:75–82. https://doi.org/10.1111/j.1600-0854.2005.00260.x

Cheever, M.L., T.K. Sato, T. de Beer, T.G. Kutateladze, S.D. Emr, and M. Overduin. 2001. Phox domain interaction with PtdIns(3)P targets the Vam7 t-SNARE to vacuole membranes. *Nat. Cell Biol.* 3:613–618. https://doi.org/10.1038/35083000

Cooke, F.T., S.K. Dove, R.K. McEwen, G. Painter, A.B. Holmes, M.N. Hall, R.H. Michell, and P.J. Parker. 1998. The stress-activated phosphatidylinositol 3-phosphate 5-kinase Fab1p is essential for vacuole function in S. cerevisiae. *Curr. Biol.* 8:1219–1222. https://doi.org/10.1016/S0960-9822(07)00513-1

Cullen, P.J. 2008. Endosomal sorting and signalling: an emerging role for sorting nexins. *Nat. Rev. Mol. Cell Biol.* 9:574–582. https://doi.org/10.1038/nrm2427

Darsow, T., C.G. Burd, and S.D. Emr. 1998. Acidic di-leucine motif essential for AP-3-dependent sorting and restriction of the functional specificity of the Vam3p vacuolar t-SNARE. *J. Cell Biol.* 142:913–922. https://doi.org/10.1083/jcb.142.4.913

Gary, J.D., A.E. Wurmser, C.J. Bonangelino, L.S. Weisman, and S.D. Emr. 1998. Fab1p is essential for PtdIns(3)P 5-kinase activity and the maintenance of vacuolar size and membrane homeostasis. *J. Cell Biol.* 143:65–79. https://doi.org/10.1083/jcb.143.1.65

Hettema, E.H., M.J. Lewis, M.W. Black, and H.R. Pelham. 2003. Retromer and the sorting nexins Snx4/41/42 mediate distinct retrieval pathways from yeast endosomes. *EMBO J.* 22:548–557. https://doi.org/10.1093/emboj/cdg062

Horazdovsky, B.F., B.A. Davies, M.N. Seaman, S.A. McLaughlin, S. Yoon, and S.D. Emr. 1997. A sorting nexin-1 homologue, Vps5p, forms a complex with Vps17p and is required for recycling the vacuolar protein-sorting receptor. *Mol. Biol. Cell.* 8:1529–1541. https://doi.org/10.1091/mbc.8.8.1529

Kaiser, C., S. Michaelis, and A. Mitchell. 1994. Methods in Yeast Genetics: A Cold Spring Harbor Laboratory Course Manual. Cold Spring Harbor Lab Press, Cold Spring Harbor, NY.

Krsmanovic, T., A. Pawelec, T. Sydor, and R. Kölling. 2005. Control of Ste6 recycling by ubiquitination in the early endocytic pathway in yeast. *Mol. Biol. Cell.* 16:2809–2821. https://doi.org/10.1091/mbc.E04-10-0941

Kvainickas, A., A. Jimenez-Orgaz, H. Nägele, Z. Hu, J. Dengjel, and F. Steinberg. 2017. Cargo-selective SNX-BAR proteins mediate retromer trimer independent retrograde transport. *J. Cell Biol.* 216:3677–3693. https://doi.org/10.1083/jcb.201702137

Legakis, J.E., W.L. Yen, and D.J. Klionsky. 2007. A cycling protein complex required for selective autophagy. *Autophagy.* 3:422–432. https://doi.org/10.4161/auto.4129

Ma, M., C.G. Burd, and R.J. Chi. 2017. Distinct complexes of yeast Snx4 family SNX-BARs mediate retrograde trafficking of Snc1 and Atg27. *Traffic.* 18:134–144. https://doi.org/10.1111/tra.12462

Marcusson, E.G., B.F. Horazdovsky, J.L. Cereghino, E. Gharakhanian, and S.D. Emr. 1994. The sorting receptor for yeast vacuolar carboxypeptidase Y is encoded by the VPS10 gene. *Cell.* 77:579–586. https://doi.org/10.1016/0092-8674(94)90219-4

Mizushima, N., T. Yoshimori, and Y. Ohsumi. 2011. The role of Atg proteins in autophagosome formation. *Annu. Rev. Cell Dev. Biol.* 27:107–132. https://doi.org/10.1146/annurev-cellbio-092910-154005

Ohsumi, Y., and Y. Anraku. 1981. Active transport of basic amino acids driven by a proton motive force in vacuolar membrane vesicles of Saccharomyces cerevisiae. *J. Biol. Chem.* 256:2079–2082.

Perera, R.M., and R. Zoncu. 2016. The Lysosome as a Regulatory Hub. *Annu. Rev. Cell Dev. Biol.* 32:223–253. https://doi.org/10.1146/annurev-cellbio-111315-125125

Schekman, R. 1985. Protein localization and membrane traffic in yeast. *Annu. Rev. Cell Biol.* 1:115–143. https://doi.org/10.1146/annurev.cb.01.110185.000555

Schu, P.V., K. Takegawa, M.J. Fry, J.H. Stack, M.D. Waterfield, and S.D. Emr. 1993. Phosphatidylinositol 3-kinase encoded by yeast VPS34 gene essential for protein sorting. *Science.* 260:88–91. https://doi.org/10.1126/science.8385367

Seaman, M.N., E.G. Marcusson, J.L. Cereghino, and S.D. Emr. 1997. Endosome to Golgi retrieval of the vacuolar protein sorting receptor, Vps10p, requires the function of the *VPS29, VPS30,* and *VPS35* gene products. *J. Cell Biol.* 137:79–92. https://doi.org/10.1083/jcb.137.1.79

Seaman, M.N., J.M. McCaffery, and S.D. Emr. 1998. A membrane coat complex essential for endosome-to-Golgi retrograde transport in yeast. *J. Cell Biol.* 142:665–681. https://doi.org/10.1083/jcb.142.3.665

Segarra, V.A., D.R. Boettner, and S.K. Lemmon. 2015. Atg27 tyrosine sorting motif is important for its trafficking and Atg9 localization. *Traffic.* 16:365–378. https://doi.org/10.1111/tra.12253

Shah, S.P., R.D. Morin, J. Khattra, L. Prentice, T. Pugh, A. Burleigh, A. Delaney, K. Gelmon, R. Guliany, J. Senz, et al. 2009. Mutational evolution in a lobular breast tumour profiled at single nucleotide resolution. *Nature.* 461:809–813. https://doi.org/10.1038/nature08489

Simonetti, B., C.M. Danson, K.J. Heesom, and P.J. Cullen. 2017. Sequence-dependent cargo recognition by SNX-BARs mediates retromer-independent transport of CI-MPR. *J. Cell Biol.* 216:3695–3712. https://doi.org/10.1083/jcb.201703015

Tarassov, K., V. Messier, C.R. Landry, S. Radinovic, M.M. Serna Molina, I. Shames, Y. Malitskaya, J. Vogel, H. Bussey, and S.W. Michnick. 2008. An in vivo map of the yeast protein interactome. *Science.* 320:1465–1470. https://doi.org/10.1126/science.1153878

Traer, C.J., A.C. Rutherford, K.J. Palmer, T. Wassmer, J. Oakley, N. Attar, J.G. Carlton, J. Kremerskothen, D.J. Stephens, and P.J. Cullen. 2007. SNX4 coordinates endosomal sorting of TfnR with dynein-mediated transport into the endocytic recycling compartment. *Nat. Cell Biol.* 9:1370–1380. https://doi.org/10.1038/ncb1656

Yamamoto, H., S. Kakuta, T.M. Watanabe, A. Kitamura, T. Sekito, C. Kondo-Kakuta, R. Ichikawa, M. Kinjo, and Y. Ohsumi. 2012. Atg9 vesicles are an important membrane source during early steps of autophagosome formation. *J. Cell Biol.* 198:219–233. https://doi.org/10.1083/jcb.201202061

Yen, W.L., J.E. Legakis, U. Nair, and D.J. Klionsky. 2007. Atg27 is required for autophagy-dependent cycling of Atg9. *Mol. Biol. Cell.* 18:581–593. https://doi.org/10.1091/mbc.E06-07-0612

Zhu, L., J.R. Jorgensen, M. Li, Y.S. Chuang, and S.D. Emr. 2017. ESCRTs function directly on the lysosome membrane to downregulate ubiquitinated lysosomal membrane proteins. *eLife.* 6:e26403. https://doi.org/10.7554/eLife.26403